Diamond Stability with Respect to Oxidation in Experiments with Minerals from Mantle Xenoliths at High P–T Parameters

E. I. Zhimulev*, V. M. Sonin**, I. I. Fedorov*, A. A. Tomilenko**, L. N. Pokhilenko**, and A. I. Chepurov*

Engineering and Technological Institute of Monocrystals, Siberian Division, Russian Academy of Sciences, Russkaya ul. 43, Novosibirsk, 630058 Russia
e-mail: egor@ns.nsb.ru
**Institute of Mineralogy and Petrography, Siberian Division, Russian Academy of Sciences, pr. Akad. Koptyuga 3, Novosibirsk, 630090 Russia*

Received June 18, 2002

Abstract—Experimental results are presented on the etching of diamond crystals in a system including silicate minerals from mantle xenoliths and C–O–H fluid at 5.5–6.0 GPa and 1450–1500°C. Slight etching patterns were established in the experiments with garnet lherzolite, eclogite, and spinel lherzolite samples. No changes in the weight and morphology of diamond crystals were detected in experiments with dunite and garnet pyroxenite samples. Water was the major component of the experimental fluid; CO_2 and CH_4 occurred in minor amounts. Hydrogen was detected in two runs, and traces of heavy hydrocarbons were noticed. Our study demonstrated that (1) diamond can in principle be etched with fluids under parameters of its thermodynamic stability and (2) the composition of fluid captured in mantle minerals is close to equilibrium with diamond. Therefore, it can be assumed that diamond is stable for an infinite time under high P–T parameters, if the equilibrium conditions are maintained.

INTRODUCTION

A hypothesis of the deep mantle origin of diamonds from kimberlites is currently regarded as the most plausible, whereas the kimberlitic magma itself is considered to be a transporting agent [1]. Taking into account the older age of most diamonds relative to their host kimberlites [2], it is reasonable to suggest that diamonds, before their capture by kimberlitic melt, occurred in a mantle environment that was inert with respect to diamond; otherwise they could not be preserved. The conditions of diamond preservation under high total pressure must, first, fit the P–T field of the thermodynamic stability of diamond; second, diamond must be incorporated in solid mantle rocks in order to prevent its recrystallization in a silicate melt; and, third, the long-term preservation of diamond requires equilibrium with the fluid phase. There are direct facts supporting these statements. Diamond crystals from mantle xenoliths entrained by kimberlites show the lowest degree of dissolution in comparison with diamonds hosted by the kimberlites themselves [3, 4]. The diamond crystals that have survived during xenolith disintegration were probably conserved in mantle rocks for the longest time [5]. For example, large diamonds from the Arkhangel'sk kimberlite pipes are mainly rounded tetrahexahedrons and rhombododecahedrons, which is indicative of their extensive dissolution. The advanced disintegration and resorption of mantle xenoliths from

the Arkhangel'sk deposits are supported by the relatively low content of the minerals accompanying the diamonds [6]. Fine crystals (<1 mm) that were found in serpentine pseudomorphs after olivine are plane-faced octahedrons almost without any signs of etching [7]. The variable degree of diamond preservation, especially in a single deposit, e.g., in the Lomonosov pipe, suggests that small diamond crystals were conserved in large olivine grains.

The objective of this work is to investigate experimentally diamond preservation in mantle mineral assemblages with natural contents of volatile components.

EXPERIMENTAL

The experiments were carried out on a multianvil high-pressure apparatus of the split-sphere type. The experimental technique was described in detail in [8]. Experiments were conducted in sealed platinum capsules at 5.5–6.0 GPa and 1450–1500°C. The high-pressure cell consisted of refractory oxides (ZrO_2, MgO, and CaO). Pressure was determined using a calibration curve based on phase transitions in Bi and PbSe at room temperature. Temperature was measured with a PtRh30/6 thermocouple. The run duration was one hour.

Table 1. Microprobe analyses of minerals from the diamond-bearing assemblages used in the experiments

Sample	SiO$_2$	TiO$_2$	Al$_2$O$_3$	Cr$_2$O$_3$	MnO	FeO	MgO	CaO	Na$_2$O	NiO	Total
YB-609/89											
Ga	41.4	0.411	17.97	6.05	0.363	7.42	20.27	5.39	0.083	–	99.36
Ol	41.06	–	–	0.067	0.118	8.77	49.42	0.035	–	0.352	99.83
Opx	58.17	0.104	0.454	0.253	–	4.89	34.95	0.746	0.135	–	99.72
YB-1467/89											
Sp	–	0.044	26.7	42.3	–	16.64	14.1	–	–	–	99.72
Ol	41.18	–	–	–	0.121	7.46	50.5	0.007	–	0.341	99.61
Opx	57.01	0.017	2.03	0.532	–	4.77	34.52	0.548	0.041	–	99.48
Cpx	54.36	0.018	2.04	1.06	–	1.48	17.14	22.24	0.87	–	99.21
YB-140/93											
Ga	41.4	0.07	15.64	10.43	0.44	7.25	21.33	3.21	0.05	–	99.83
Ol	41.53	–	–	0.03	0.102	7.2	51.07	0.007	–	0.356	100.29
Crt	–	0.006	37.25	31.37	–	14.08	17.05	–	–	–	99.76
RV-3											
Ga	42.01	0.185	22.18	0.407	–	11.18	17.96	5.05	0.055	–	99.03
Cpx	54.85	0.099	1.55	0.083		3.28	16.71	21.34	1.1	–	99.02
YB-25/84											
Ga	41.54	0.323	22.11	0.46	0.465	9.95	18.61	6.2	0.075	–	99.75
Cpx	54.84	0.189	2.36	0.439	–	2.92	15.85	20.58	1.84	–	99.02

Note: Samples: RV-3/91, eclogite; YB-140/93, dunite; YB-609/89, garnet lherzolite; YB-1467/89, spinel lherzolite; and YB-25/84, garnet pyroxenite.

The compositions of natural diamond-bearing assemblages corresponding to the dunite, garnet lherzolite, spinel lherzolite, and garnet pyroxenite from the Udachnaya-Vostochnaya kimberlite pipe in Yakutia and to the eclogite from the Roberts Victor kimberlite pipe in South Africa were used as starting silicate mixtures. The chemical compositions of minerals are given in Table 1. Natural plane-faced and sharp-edged octahedral and synthetic cuboctahedral diamond crystals were used in this study.

After experiments, the platinum capsules with samples were placed into a special unit connected with a chromatographic system. The capsules were heated to 150°C and then pierced with a striker. The released gas was analyzed using the method described in [9, 10]. The molecular composition of fluid in equilibrium with diamond under experimental P–T conditions was calculated for the H/(O + H) ratio determined after the run by the minimization of the free energy of the system regarding the fluid as an ideal mixture of real gases. The computational technique and the sources of the thermodynamic data are given in [8].

After experiments the diamond crystals were successively washed in HF, HCl, and an oxidizing mixture consisting of K$_2$Cr$_2$O$_7$ and H$_2$SO$_4$. The loss of crystal mass was determined by weighing with an accuracy of ±0.01 mg. The crystal morphology was examined under MBS-10 and MBI-15 optical microscopes and a JSM-35 scanning electron microscope.

RESULTS

The experimental conditions and results are given in Table 2. The melting temperature of the silicate samples was never attained. The silicate minerals were analyzed after experiments with an electron microprobe, which showed that their chemical compositions did not change. Diamonds from the samples of garnet lherzolite and eclogite were partly etched. The diamonds of the garnet lherzolite association lost 0.04 mg (2.8 wt %). The most substantial weight loss was detected in diamonds from runs with eclogite: 7.0 and 3.2 wt %. The greater loss was found in the experiment in which pyroxene prevailed over garnet. In run 7-9-99 with spinel lherzo-

Table 2. Conditions and results of experiments in the presence of natural minerals from diamond-bearing mantle assemblages

Run number	Sample	Composition	Weight, mg (%)	Diamonds	Starting weight, mg	Final weight, mg	Etch figures
4-36-97	Dunite YB-140/93	*Ol*	108.6 (93)	1, natural	0.57	0.57	None
		Ga	8.2 (7)				
7-28-98	Eclogite RV-3/91	*Cpx*	67.7 (60)	1, natural	0.57	0.53	Negative trigons and parallel striation
		Ga	45.1 (40)				
7-9-99	Spinel lherzolite YB-1467/89	*Ol*	95.0 (95)	1, natural	1.27	1.27	None
		Opx	3.0 (3)				
		Sp	2.0 (2)				
7-14-99	Garnet pyroxenite YB-25/84	*Ga*	73.45 (83)	2, synthetic	1.57	1.57	None
		Cpx	15.0 (17)				
8-25-99	Garnet lherzolite YB-609/89	*Ol*	80.37 (82.7)	2, synthetic	1.43	1.39	Negative trigons, parallel striation, and serrate sculpture
		Opx	6.9 (7.1)				
		Ga	9.95 (10.2)				
8-30-99	Eclogite RV-3/91	*Ga*	51.5 (50.7)	2, synthetic	1.54	1.49	Faces (111): negative trigons, parallel striation, and serrate sculpture; faces (100): square etch pits
		Cpx	50.0 (49.3)				
8-37-99	Spinel lherzolite YB-1467/89	*Ol*	86.40 (81.3)	2, synthetic	1.48	1.48	Faces (111): negative trigons, parallel striation, and serrate sculpture; faces (100): square etch pits; imprints of solid phases
		Opx	15.15 (14.3)				
		Sp	4.7 (4.4)				

lite, no signs of diamond crystal etching were detected. In run 8-37-99 the silicate material contained more orthopyroxene and spinel and less olivine than that of run 7-9-99. Only a slight change of face micromorphology was detected in this run without any measurable weight loss. The weight and morphology of the crystals did not change in the experiments with dunite and garnet pyroxenite.

Changes in the micromorphology of diamond crystals included the appearance of triangular etch pits, both flat-bottomed and pyramidal, showing a negative orientation to the (1̄11) faces (Fig. 1). Square pyramidal etch pits with sides parallel to the edges of octahedral faces were formed on the (100) faces. Parallel striation was seen in places near the edges of octahedral faces, and a serrate sculpture (terminology of Orlov [5]) was formed near the edges between the octahedral and cubic faces (Fig. 2). The reentering angle between particular dents equals 60°. The edges of the steps making up this sculpture, as well as the walls of the etch pits are oriented parallel to the surfaces of a trigon-trioctahedron. In addition, an unusual sculpture consisting of flattened hillocks of varying size with polygonal (largely rectangular) contours independent of the face symmetry was found in run 8-37-99 (Fig. 3). These figures are probably imprints of the solid silicate grains that screened the crystal surface during etching.

Fig. 1. Triangular etch pits on the (111) face of a diamond crystal, run 8-25-99. Magnification 120.

Chromatographic analysis showed that water was the major fluid component in the experiments, and CO_2
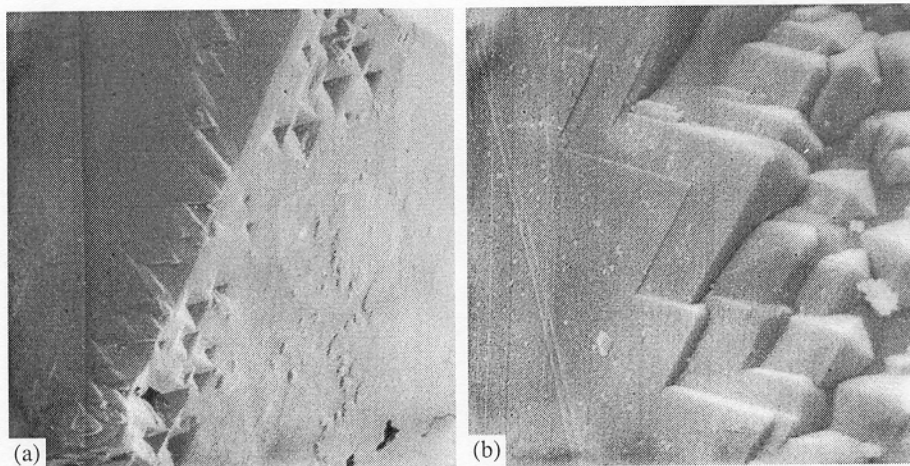
Fig. 2. Serrate etch sculpture on the (111) face and square pyramidal etch pits on the (100) face of diamond crystals from (a) run 8-30-99, magnification 200, and (b) run 8-37-99, magnification 1330.
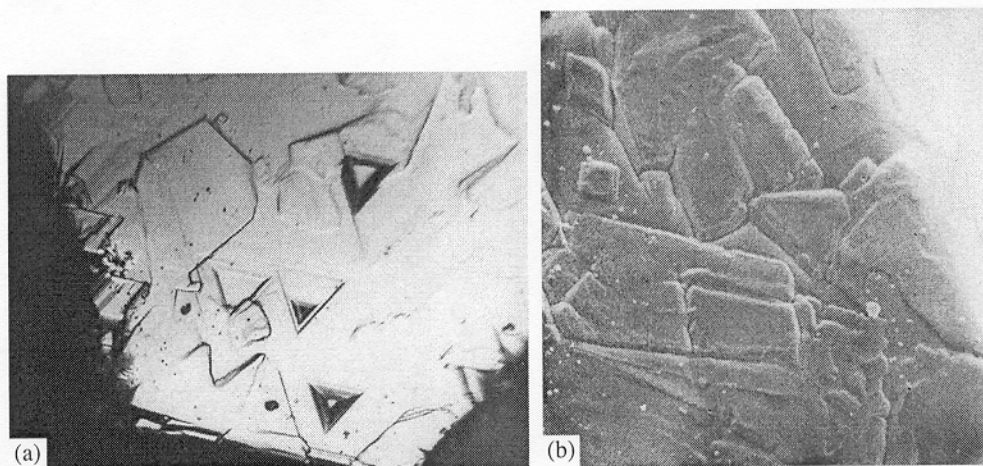

Fig. 3. Flattened polygonal hillocks and triangular etch pits on (a) the (111) face, magnification 240, and (b) the (100) face of diamond crystals, magnification 320; run 8-37-99.

and CH_4 occurred in much smaller amounts. Hydrogen was detected in two runs. In addition, traces of heavy hydrocarbons were noticed (Table 3). The calculated compositions of fluid in equilibrium with diamond under the experimental parameters are shown in Table 4.

DISCUSSION

The solidus of dry mantle rocks lies at high temperatures (Fig. 4). According to these data, only alkaline basic rocks could be melted at the parameters of our experiments. The amount of water was insufficient to significantly lower the melting temperature of the samples (Table 3), because the addition of <5 wt % H_2O lowers melting temperatures in silicate systems by no more than 100–150°C [19, 20]. Therefore, the samples

in our experiments were not subjected to melting. Thus, it can be concluded that the partial etching of diamond crystals was induced by the fluid that occurred initially in the silicate minerals and was captured during sample preparation. However, since etching did not take place in all runs, it was probably controlled by the fluid composition. It can be suggested that etching did not occur, if the fluid composition was originally close to equilibrium with diamond. In contrast, if the fluid composition departed from equilibrium with diamond, slight etching was observed.

The resulting etch figures are similar to the sculptures described on natural crystals [5, 21, 22] and reproduced previously by diamond etching in silicate melts of alkali basalt [23–25], lamproite [26], and kimberlite [27]. The chromatographic results testify to a relatively

Table 3. Results of the chromatographic analysis of experimental products, mg/kg (mol %)

Run number	CO_2	H_2O	CO	H_2	CH_4	C_2H_4
4-36-97	50 (1.8)	1100 (97.9)	0	0	0	0
7-28-98	160 (2.3)	2400 (84.2)	0	40 (12.6)	20 (0.8)	4 (0.1)
7-9-99	0	390 (99.7)	0	0	1 (0.3)	0
7-14-99	410 (4.4)	3600 (95.5)	0	0	2 (0.06)	0.3 (0.005)
8-25-99	100 (1.1)	2600 (69.6)	0	120 (28.9)	10 (0.3)	6 (0.1)

Run number	C_3H_8	C_4H_{10}	C_5H_{12}	C_2H_2	H/(O + H)
4-36-97	3 (0.1)	7 (0.2)	0	0	0.67
7-28-98	0	1 (0.01)	1 (0.01)	0	0.69
7-9-99	0	0	0	0	0.67
7-14-99	1 (0.01)	0.2	0	0	0.65
8-25-99	2 (0.02)	0.8 (0.005)	0.7 (0.005)	0	0.73

narrow range of H/(O + H) values and, correspondingly, oxygen fugacity in the fluid phase ($-\log fO_2 = 5.0$–5.7). Nevertheless, in the runs where diamond etching was detected, the fluid was somewhat more reduced (Table 3). The presence of hydrogen and the absence of CO were noticed. It can therefore be suggested that diamond etching was caused by the reaction of oxidation by water, $2H_2O + C = CO_2 + 2H_2$. The etching ceased when equilibrium was achieved in the system (this likely occurred rather rapidly). This is confirmed by the very small weight losses of diamond despite the high temperature of the experiments.

The oxygen fugacity in the fluid phase under our experimental conditions lay between the IW and CCO curves and close to the CCO values [8]. The lower values in comparison with the CCO buffer are due to the fact that the equilibrium curve is shifted in the C–H–O system toward more reduced values relative to the C–O system, and this shift depends on the hydrogen content [28].

According to the chromatographic data, H_2O and CO_2 are the main components of mantle fluid, and the maximum amount of water is 80–90 mol % [29]. The most reduced fluid was found in dunite and harzburgite samples, and the most oxidized, in spinel peridotites. Garnet lherzolites, pyroxenites, and eclogites occupy an intermediate position. However, the oxygen fugacity of fluid captured in all samples of mantle rocks falls within the IW–CCO range. Direct electrochemical measurements of the redox state of mantle samples yielded similar results, and inclusions in diamond and the least oxidized peridotites have an oxygen fugacity at the level of the IW buffer [30]. Oxidized fluid species (H_2O and CO_2) are stable in the upper mantle, whereas methane becomes stable within deeper zones near the boundary between the upper mantle and the transitional zone [31]. The oxidation of mantle rocks up to the CCO level is considered as the main trend of mantle evolution during the formation of the ancient lithosphere.

Table 4. Calculated composition (mol %) of C–O–H fluid in equilibrium with diamond at 5.5 GPa and 1500°C

Component	H/(O + H) = 0.65	H/(O + H) = 0.67	H/(O + H) = 0.69	H/(O + H) = 0.73
H_2O	84	85	82	79
CO_2	8	5.2	4.3	1.6
CO	1.3	1.1	0.96	0.62
CH_4	4.1	5.1	8.6	14
H_2	2.3	2.6	3.3	4.2
C_2H_2	1.2E–05	1.4E–05	1.8E–05	2.4E–05
C_2H_4	5.4E–03	5.6E–03	1.1E–02	1.8E–02
C_2H_6	4E–02	4.9E–02	0.11	0.22
C_3H_8	9E–05	1E–04	3.8E–04	8E–04
C_4H_{10}	1.5E–04	1.5E–04	8E–04	1.9E–03
O_2	3.7E–11	2.4E–11	1E–11	7.5E–12
$\log fO_2$	–5.0	–5.2	–5.3	–5.7

Our study has shown that diamond etching with fluid is principally possible under the parameters of its thermodynamic stability; however, the composition of fluid captured in mantle minerals is close to equilibrium with diamond. Taking into account the minor extent of etching and its absence in some mantle samples, one can suggest that diamond is stable for an infinite time
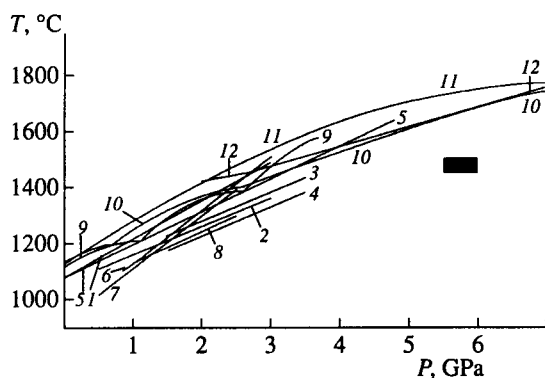
Fig. 4. Dry solidi of natural mantle-derived rocks according to published data. (*1, 2*) Olivine tholeiite and alkali olivine basalt, respectively [11]; (*3, 4*) high-alumina quartz tholeiite and basaltic andesite [12]; (*5*) olivine tholeiite MN5 [13]; (*6–8*) garnet clinopyroxenite R392, spinel–garnet websterite R394, and garnet–plagioclase clinopyroxenite R130 [14]; (*9*) peridotite HK66 [15]; (*10*) natural lherzolite KLB-1 [16]; (*11*) peridotite sample PHN1611 [17]; and (*12*) peridotite KR4003 [18]. The filled rectangle shows the *P–T* parameters of our experiments.

under high *P–T* parameters, if equilibrium conditions are maintained.

REFERENCES

1. N. N. Sarsadskikh and V. S. Rovsha, Zap. Vses. Mineral. O–va **89** (4), 392 (1960).

2. S. H. Richardson, J. W. Harris, and J. J. Gurney, Nature **366**, 256 (1993).

3. V. N. Kvasnitsa, N. N. Zinchuk, and V. I. Koptil, *Typomorphism of Diamond Microcrystals* (Nedra, Moscow, 1999) [in Russian].

4. V. P. Afanas'ev, É. S. Efimova, N. N. Zinchuk, and V. I. Koptil', *Atlas of the Morphology of Russian Diamonds* (Scientific Publishing Center UIGGM, Novosibirsk, 2000) [in Russian].

5. Yu. L. Orlov, *The Diamond Morphology* (Akad. Nauk SSSR, Moscow, 1963) [in Russian].

6. N. V. Sobolev, N. P. Pokhilenko, V. P. Grib, *et al.*, Geol. Geofiz., No. 10, 84 (1992).

7. V. D. Khar'kiv, N. N. Zinchuk, and V. M. Zuev, *The History of Diamond* (Nedra, Moscow, 1997) [in Russian].

8. A. I. Chepurov, I. I. Fedorov, and V. M. Sonin, *Experimental Modeling of Diamond Formation* (Scientific Publishing Center UIGGM, Novosibirsk, 1997) [in Russian].

9. N. Yu. Osorgin, *Chromatographic Analysis of Gas Phase in Minerals (Methods, Equipment, and Metrology)* (Institute Geol. Geophys., Siberian Division, Russian Academy of Sciences, Novosibirsk, 1990) [in Russian].

10. N. Yu. Osorgin, I. I. Fedorov, V. M. Sonin, and D. G. Bagryantsev, in *Proceedings on Genetic and Experimental Mineralogy* (Siberian Division, Russian Academy of Sciences, Novosibirsk, 1995), Vol. 11, pp. 74–80 [in Russian].

11. D. H. Green and A. E. Ringwood, Contrib. Mineral. Petrol. **15**, 103 (1967).

12. T. H. Green and A. E. Greenwood, Contrib. Mineral. Petrol. **18**, 105 (1968).

13. L. H. Cohen, K. Ito, and G. C. Kennedy, Am. J. Sci. **265**, 475 (1967).

14. A. J. Irving, J. Petrol. **15**, 1 (1974).

15. E. Takahashi and I. Kushiro, Am. Mineral. **68**, 859 (1983).

16. E. Takahashi, J. Geophys. Res. **91**, 9367 (1986).

17. C. M. Scarfe and E. Takahashi, Nature **322**, 354 (1986).

18. M. J. Walter, J. Petrol. **39**, 29 (1998).

19. T. H. Green, Contrib. Mineral. Petrol. **34**, 150 (1972).

20. I. A. Nicholls and A. E. Ringwood, J. Geol. **81**, 285 (1973).

21. A. A. Kukharenko, *Diamonds of the Urals* (Gosgeoltekhizdat, Moscow, 1955) [in Russian].

22. Z. V. Bartoshinskiĭ and V. N. Kvasnitsa, *Crystal Morphology of Diamond from Kimberlites* (Naukova Dumka, Kiev, 1991) [in Russian].

23. A. I. Chepurov, A. F. Khokhryakov, V. M. Sonin, *et al.*, Dokl. Akad. Nauk SSSR **285**, 212 (1985).

24. V. M. Sonin, E. I. Zhimulev, I. I. Fedorov, and N. Yu. Osorgin, Geokhimiya, No. 4, 451 (1997) [Geochem. Int. **35**, 393 (1997)].

25. V. M. Sonin, E. I. Zhimulev, I. I. Fedorov, *et al.*, Geokhimiya, No. 3, 305 (2001) [Geochem. Int. **39**, 268 (2001)].

26. A. F. Khokhryakov and Yu. N. Pal'yanov, Mineral. Zh., No. 1, 14 (1990).

27. V. M. Sonin, E. I. Zhimulev, A. I. Chepurov, and V. P. Afanas'ev, Izv. Vyssh. Uchebn. Zaved., Geol. Razved., No. 1, 60 (2002).

28. A. A. Kadik and O. A. Lukanin, *Degassing of the Upper Mantle during Melting* (Nauka, Moscow, 1986) [in Russian].

29. L. N. Pokhilenko and A. A. Tomilenko, *Proceedings of the 14th All-Russia Conference on Experimental Mineralogy* (Chernogolovka, 2001), p. 276.

30. A. A. Kadik, Vestn. OGGGGN RAN, No. 4, 65 (1999).

31. I. D. Ryabchikov, Vestn. OGGGGN RAN, No. 3, 142 (1999).